Joint Special Interest Group meeting between euspen and ASPE
Advancing Precision in Additive Manufacturing
Ecole Centrale de Nantes, France, September 2019
www.euspen.eu

Improving metal additive manufacturing part design and final part precision using feedback from X-ray computed tomography.

Markus Baier[1], Mirko Sinico[2,3], Umberto Paggi[2,4], Ann Witvrouw[2,3], Lore Thijs[4], Wim Dewulf[2], Simone Carmignato[1]

[1]Department of Management and Engineering, University of Padova, 36100 Vicenza, Italy
[2]Department of Mechanical Engineering, KU Leuven, 3001 Leuven, Belgium
[3]Member of Flanders Make - Core lab PMA-P, KU Leuven, 3001 Leuven, Belgium
[4]3D Systems Leuven, 3001 Leuven, Belgium

markus.baier@unipd.it

Abstract
Additive metal manufacturing processes, such as laser powder bed fusion, still show difficulties when producing overhang features or internal structures such as channels or bores. Channels are often mutilated by sag defects and dross formation at their upper part, when the channel-axis is close to parallel to the base plate and in the particular case when support structures cannot be used as it would be impossible to remove them after the build. The problem is still not completely solved, although various design guidelines have been developed for various processes and materials in use. So far, a general approach is to tweak the processing parameters or to orient the design on the build plate to reduce downfacing regions at the most critical features of the parts. This work proposes to use feedback from X-ray computed tomography measurements and a new evaluation approach for the additive manufacturing process-chain to obtain improved geometrical accuracy of internal channels. Preliminary results on the evaluation are presented, with the future scope of reducing sag and dross defects by adapting the channels and bores during the design stage.

Laser Powder Bed Fusion, Accuracy of internal channels, Feedback for design, Feedback for AM process, X-ray Computed Tomography

1. Introduction

Despite the increasing use of metal additively manufactured (AM) parts over a wide spectrum of industries, the precision of metal AM parts is still a major problem that hinders the full exploitation of the possibilities offered by this rather new manufacturing technique. One of the most commonly used processes is laser powder bed fusion (LPBF), which uses a laser to selectively melt metal powder particles together, to create the part in a layer by layer approach from a design file. Due to the nature of the build process it is inevitable that the final parts undergo thermal gradients and are fully immersed in the powder after finishing the print. This has a direct impact on the borders of the part and can cause deviations from the design file as well as highly complex surface textures, since particles in the direct vicinity of the border hatches can be partially molten by the traversing laser and thus will be attached to the parts surface. This effect becomes much more prominent in overhanging regions, which means the laser beam passes over a section of the powder-layer under which only loose powder and no supports or a previous laser track is present. In this case, not only the particles in the vicinity, but the powder of several-layers can be affected by the accumulation of heat in this area and so called "sag" and "dross" defects occur [1]. To prevent this, various design guidelines have been developed in the past for various processes and materials in use [2] and to date it is common to adapt the process parameters accordingly, whenever the laser track is close to the borders of the part [3, 4]. This kind of approach, however, is very time consuming, as it is often only possible to find the right parameter sets with trial and error studies. Furthermore, these studies concentrate only on the scope of the build process itself i.e. placement of the parts in the optimal way on top of the base plate, selection of the right build parameters and so forth, but the problems they aim to prevent are already present in the design stage of the part. In recent studies, X-ray computed tomography (CT) has been applied to visualise and measure the shape and the surface roughness of internal channels of metal AM parts and to determine dimensional features [5, 6]. Trying to get a step further, this work aims for attracting attention to the various possibilities offered by CT to not only verify metal AM parts, but also to give feedback to different stages of the AM process including part design, and to show the need of other approaches to tackle the hurdles of AM processes. This will help getting one step ahead in providing first time right parts, built with LPBF.

For this reason, "spyglass" shaped parts (see Figure 1) consisting of hollow cylinder sections with different internal diameters, connected by conical sections, as well as reference cubes, were designed, printed and examined without any further post-processing despite removal of the residual powder. The main measurements of the full part is conducted with CT, including a subsequent analysis of the overall part dimensions and properties as porosity and inclusions. Furthermore, image stacks perpendicular to the cylinder axes are extracted from the CT volumes to further assess the sag and dross formation in the upper parts of the internal channels. Measurements of the surface roughness with a contact stylus probe and measurements of the density of the reference cubes with the Archimedes method are carried out to provide complementary information to the CT results.

2. Design and manufacturing of the test part

The "spyglass" test part consisting of eight hollow cylinders and inter-connecting frusta with different diameters is designed considering proper measurability with CT. The parts are built in

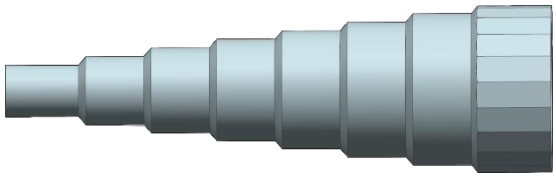

Figure 1. Rendering of the artefact with internal diameters that range from 2 mm (left side) to 16 mm (right side) and a wall thickness of 2 mm. The overall length of the part is 75 mm.

horizontal, vertical and at 45° with respect to the base plate, without any supports inside the cylinders, and are manufactured with a new Aluminium alloy powder (3D Systems LaserForm© AlSi7Mg0.6) on a DMP ProX 320 machine with preliminary machine parameters. Additionally, a reference cube is printed next to each test part to monitor the density across the baseplate. Figure 1 shows a rendering of the part with an inner cylinder diameter starting from 2 mm at the left side up to 16 mm at the right side, whereupon the diameter increases stepwise by 2 mm. The wall-thickness of the part is reduced to only 2 mm to make sure the whole part can afterwards be analysed properly with CT. The outer shape of the last cylindrical section on the right is changed from a cylindrical to a polygonal shape to achieve flat surfaces with certain inclinations versus the base plate, allowing to conduct surface roughness measurements. After the build, only the residual powder and the supports between part and base plate are removed and no further post-processing is applied.

3. Measurement and characterisation methods

For the characterisation of the parts, the main system is CT as it yields a very high information density in a single scan. In addition, density analysis on the reference cubes with the Archimedes method and surface roughness measurements with a contact profilometer are carried out.

3.1. Measurement with X-ray computed tomography

The spyglass part is centred on the rotary table of the *Nikon XTH 225ST* µ-CT machine, standing upright on the biggest cylinder with the cylinder axes in parallel to the vertical direction. This allows to move the part very close in front of the source and thus a very small voxel size of 10.5 µm is achieved, as the parts features are magnified onto the flat-panel detector due to the cone beam geometry. However, due to the height of the part standing upright, it is necessary to carry out separate scans for each cylinder section including an overlap between the different scans, allowing for registration and stitching of the single volumes together into one containing the full part, once the scans are finished. The parameters of the scans are optimised for the two extremes of the part i.e. the section with the smallest and the biggest diameter and are fixed to a voltage of 130 kV and a power of 6 W for each single scan, to ease the registration afterwards and to be able to run the scans as a batch. In addition, the acquisition of a reference sample containing calibrated features is conducted to be able to compensate for possible errors during the scans [7]. After the scanning, each CT volume is reconstructed with the same parameters and subsequently loaded in the analysis and visualization software VGStudio MAX 3.1 (Volume Graphics GmbH) for further processing, including registration of the single volumes. After the full part is reconstructed, the surface of the part is determined. Subsequently, a region of interest (ROI) is created from the determined surfaces and a porosity analysis is conducted. Within the same ROI, an inclusion analysis is performed to investigate possible alien material particles stemming from either the raw powder, or contaminations inside the AM machine. The full part is re-aligned against the .STL file with a best fit method, using only the three smallest cylinders as reference for alignment, as in particular the small inner channels are of interest and the bigger channels are highly deformed in vertical direction. Subsequently, a deviation to nominal analysis is performed, to investigate the overall deviations between the printed part and the design file.

In an additional step, image stacks for each cylinder diameter are extracted perpendicular to the cylinder axes, to obtain cross sections of the nominal cylinder and the actual as printed part. For each cylinder section, 780 slices with one voxel distance are extracted and further processed with an in house developed evaluation algorithm. The final goal is to give feedback to the design of the channels shape to prevent the occurrence of sag and/or dross formation in overhanging regions, however it proves very difficult to find some theoretical information approaching this problem. For this reason, only preliminary results will be presented here, as this method is still part of ongoing research and external input is necessary to determine the final parameters which can be feed to the design.

3.2. Density analysis of the reference cubes.

The density of the reference cubes is evaluated with Archimedes method and compared to the theoretical maximum density for the solid metal. In addition, a side of the cubes is polished and characterised with an optical microscope to investigate porosity and inclusions. Furthermore, an energy dispersive X-ray (EDX) analysis is conducted with a scanning electron microscope *FEI XL30 FEG* (SEM) to determine the chemical composition of the impurities.

3.3. Surface roughness measurements

Surface profiles are taken with a *Taylor Hobson Form Talysurf 120L surface analyzer* along the flat edges in direction of the cylinder axis and perpendicular to the lay to gain information about the angular dependence of the surface roughness. Profiles are also taken on the reference cubes, on the top with tracing direction perpendicular to the lay and on the side parallel to the build direction.

4. Results and discussion

From the results obtained by the different methods described in section 3 some very useful information can be extracted regarding overall performance of the machine, but also directions to improve both process and design. The contact surface roughness measurements show a strong dependence between the determined values and the facets inclination against the build plate. As a first quantification Figure 2 shows the obtained mean *Ra* values for the different facets with the corresponding standard deviation of the measurements, whereupon the roughness on downfacing surfaces is always higher than on top surfaces. Furthermore, the roughness steadily decreases from surfaces parallel to the build plate to surfaces vertical to the build direction, which agrees with the values obtained on the reference cubes (Figure 2 inset). However, especially for AM parts and surfaces, this kind of measurements provide only a limited amount of information for part and process improvement but can help to find a first direction.

Looking at the results obtained from the CT measurements, it quickly becomes clear how limited standard measurements are with respect to the evaluation of AM parts [8]. In the following only the results for the most critical case, the horizontally printed “spyglass”, are explained in more detail. Figure 3 shows a 3D rendering of the porosity obtained from the analysis of the fully reconstructed artefact volume and shows a strong correlation between the distribution of the pores and the shape of the parts owing the change in the hatch strategy. The mean distance between the parts’ surface and the pores is 151 µm.

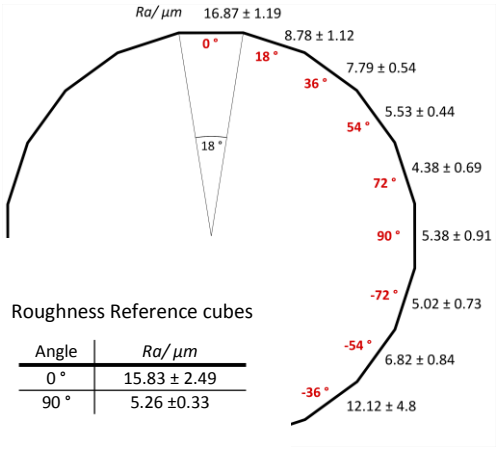

Figure 2. Obtained surface roughness values *Ra* depending on the angle between the surface and the base plate. Values decrease from *0* ° to *90* ° for up-facing as well as down-facing surfaces. The table in the inset shows the *Ra* values obtained at the top and side surface of the reference cubes.

This could be caused either by a non-optimal transition between the contour hatching and the bulk hatching, or by defects that occurs at the beginning and ending of hatching vectors in the bulk, where the melt pool is not in a steady state condition.

The density values of the reference cubes received by Archimedes method show an average porosity of 0.4 %, which appears high. However, the outcome of Archimedes method suffers from high errors especially for as built AM parts [7], because for example small air bubbles can stick on the surface of the part. In contrast, the overall volume fraction of the porosity obtained with CT is 0.11 % which relates to a part density of 99.89 %. This value, however, is an overestimation which is due to the fact, that the resolution of the CT scan was too low to detect smaller pores, caused by the trade-off to measure the entire part [7]. Furthermore, the registration of the different parts has also an influence, as there is a change of grey values throughout the stitched volume which directly influences the selection of the threshold value to separate material from porosity grey values. This is confirmed when comparing the overall porosity of the fully reconstructed part with the mean porosity obtained from the porosity analysis performed on the separate volumes with the same evaluation approach. In this case the mean part density is 99.87 %, which is slightly lower, however it shows the registration has only a small influence on

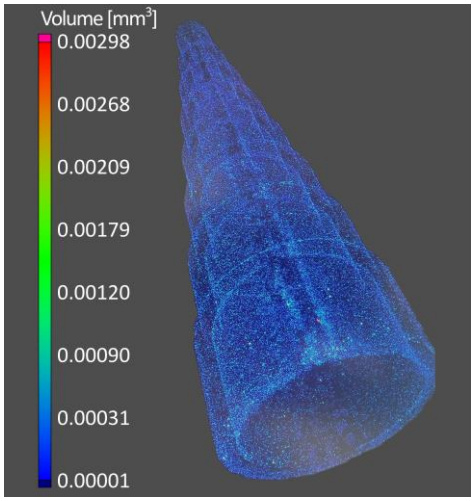

Figure 3. Rendering of the determined porosity inside the fully reconstructed volume. The volume of the pores is colour coded by the colour-bar on the left. The distribution of the pores strongly imitates the shape of the part, meaning the majority lies between surface and bulk hatch strategy.

the outcome. Looking at the mean pore diameter of around *50 µm,* it can be deduced that the print parameters are already quite optimised to achieve high part densities as there are almost no bigger pores. The inclusion analysis revealed 0,03 % of alien material inside the full part which has a higher density than the aluminium powder and by EDX analysis it could be identified as Zn particles with a mean diameter of 85 µm being the result of contaminations from a previous build job carried out on the same machine.

The deviation of the printed part from the CAD is shown in Figure 4. At the first glance, it appears that the deviations for smaller internal diameter are much lower, compared to the bigger diameters, however this is only true for external shapes.

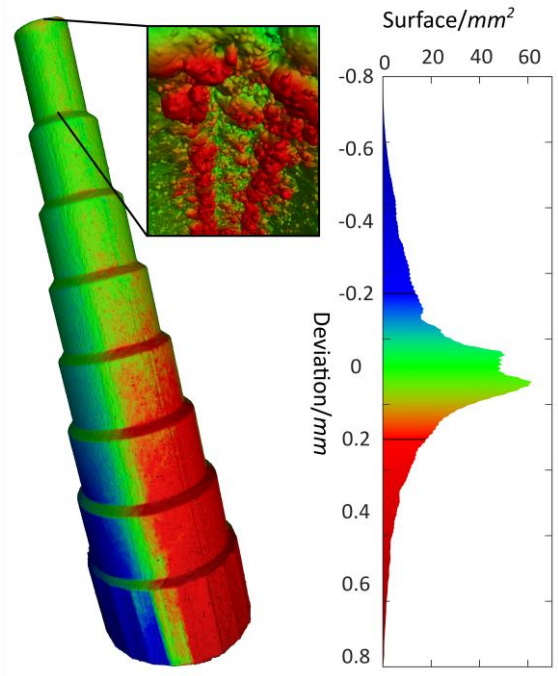

Figure 4. Deviation to nominal analysis of the fully reconstructed spyglass part. The histogram on the right shows the surface area with respect to the deviation from the .STL file in the colours of the rendered part. The inset on the top shows the internal channel topography in the overhanging region exhibiting large sag and dross formation.

When looking at the small inset in the figure it becomes clear that in particular the small channels are prone to big relative deviations due to sag and dross formation in the overhang regions inside the channels, whereas the deviations in the case of the sections with channel diameters of more than 8 mm show a totally different mix of errors and the amount of deviation is mainly governed by deformations caused by residual stresses built up during the build of the part. This implies the necessity to apply different approaches when improvement of part and process of AM parts is desired and especially feedback for design is of high interest, as the amount of feedback which can be drawn from the results discussed previously is somewhat limited due to the high complexity and enmeshment of the various sources causing erroneous parts. For this reason, first results obtained with a new approach, which is still being refined and further developed, are pointed out as even the preliminary results can already augment the feedback in particular for the design stage. Figure 5 shows the results of the evaluation of the upper semi-cylinder of the internal channels with a diameter of 2 mm rolled out on a plane. The surface plot on the top shows the maximum deviation in radial direction from the nominal cylinder radius across the length of the cylinder. The graph shows high fluctuations of the deviations with a strong dependence on the angle. The colour coding of the graph enables also the separation of two main areas, connected by a

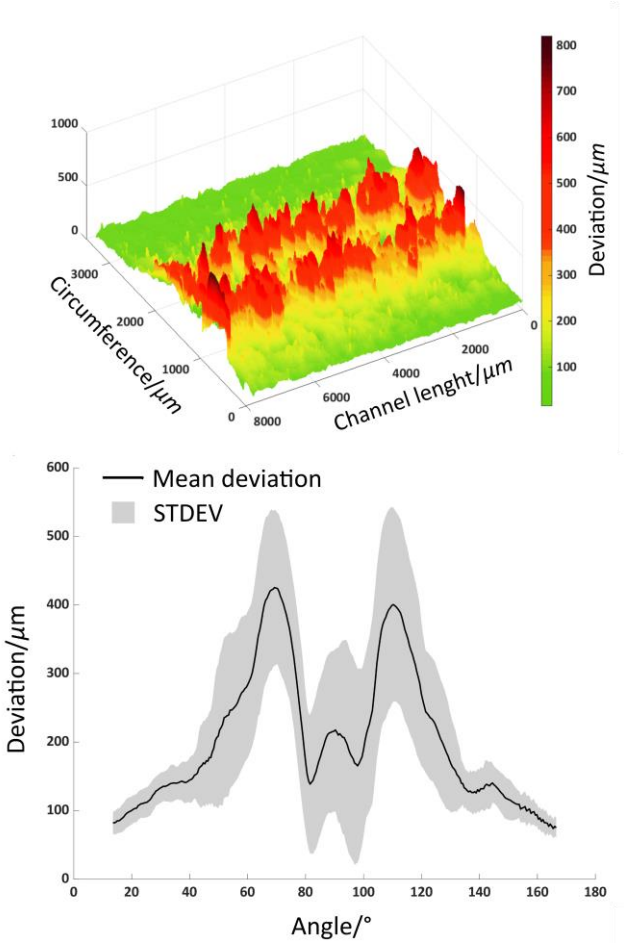

Figure 5. Preliminary results of the analysis of the sag and dross formation on the ceiling of the inner channels with 2 mm diameter. The graph on top shows the deviation from the nominal value along the cylinder circumference. The graph on the bottom shows the calculated mean deviation against the angle of the top semi-cylinder of all cross-sections including the standard deviation.

very small intermediate phase, which are influenced by different amounts of sag and/or dross formation. The first area, with deviations of up to 150 µm (green), is mainly caused by sag formation and shows very low fluctuations. In contrast, the second area is a superposition of sag- and dross-formation, while the increase of the deviation in this area is majorly governed by dross-formation. In this area the deviation shows peaks symmetrically distributed around the vertical direction. In between the peaks, the deviation is suddenly drastically reduced, which is due to the fact, that the previous layers were prone to huge errors and thus serve as self-formed supports for the subsequent layers. This behaviour is confirmed by the graph on the bottom, showing the mean deviation from the nominal cylinder accompanied by its standard deviation plotted against the angle. The areas with considerable low standard deviation nicely correspond to the first area which is governed by a more linear error (sag-defect), while the areas with high standard deviation perfectly mirror the turbulent nature of the dross-formation. Furthermore, the graph reveals that both peaks are symmetric in a distance of around 20 ° from the vertical axis, and the variation in the area between the peaks is in contrast mainly governed by sag- rather than dross-formation. Nevertheless, right in the centre between the peaks a new increase in deviation indicates, that the self-supporting nature is quite limited to a small area very close to the big deviations. In addition, the analysis of the channels with bigger inner diameters reveal the same behaviour and in particular the peaks appear in all cases at the same angular distance from the vertical direction. However, with increasing inner diameter additional error sources come into play, as deformation due to residual stresses or lack of sufficient supports, which highly increases the complexity of the factors contributing to the discrepancies.

5. Conclusions

In a nutshell, this article presents only a small part of the possibilities of computed tomography to provide useful information for AM processes and also a first attempt to give directly feedback to the design stage of AM parts.

The results revealed a strong anisotropy in the distribution of porosity due to a weak overlap between the different hatch strategies which have been applied to manufacture the investigated part.

Furthermore, the deviation to nominal analysis revealed a strong dependence between the channel diameter and the deformation due to residual stresses, but also large deviations inside the smaller channels which are caused by other processes during the printing of the part.

In addition, preliminary results of the investigation of the internal channels with a new approach enabled a deeper insight into the nature of the deviations, which allows a separation of the deviation into two areas and showed a strong dependence between the dross-formation and the angle of inclination which is more importantly also independent on the channel diameter.

Future work will focus on exploiting the obtained results to further improve the approach for the evaluation of error sources in overhang surfaces allowing for better separation of the contributing factors. Ultimately, the final goal is proposing a direct feedback for the design stage, ensuring a step ahead on the path to first time right additive manufactured metal parts.

Acknowledgements

This research was funded by The EU Framework Programme for Research and Innovation - Horizon 2020 - Grant Agreement No 721383 within the PAM² (Precision Additive Metal Manufacturing) research project. We are grateful to Stijn Schoeters for the development of the in-house code used to evaluate the surface roughness.

References

[1] Duda T and Venkat Raghavan L. 2018 3D metal printing technology: the need to re-invent design practice. AI & SOCIETY **33.2** 241-252

[2] Kranz J, Herzog D, Emmelmann C, 2015 Design guidelines for laser additive manufacturing of lightweight structures in TiAl6V4. Journal of Laser Applications. **27**(S1), S14001.

[3] Cloots M, Zumofen L, Spierings A B, Kirchheim A, Wegener K, 2017 Approaches to minimize overhang angles of SLM parts. Rapid Prototyping Journal. **23**(2), 362-369

[4] Mertens R, Clijsters S, Kempen K, Kruth J P 2014 Optimization of Scan Strategies in Selective Laser Melting of Aluminum Parts With Downfacing Areas. Journal of Manufacturing Science and Engineering. **136**, DOI:10.1115/1.4028620.

[5] Snyder J C, Stimpson C K, Thole K A, Mongillo D J, 2015 Build direction effects on microchannel tolerance and surface roughness. Journal of Mechanical Design. **137**(11), 111411.

[6] Xu D, Cheng F, Zhou Y, Matalaray T, Xian Lim P, Zhao L, 2019 Process optimization: internal feature measurement for additive-manufacturing parts using x-ray computed tomography. 40, DOI:10.1117/12.2511429.

[7] Kruth J P, Bartscher M, Carmignato S, Schmitt R, De Chiffre L, Weckenmann A, 2011 Computed tomography for dimensional metrology, CIRP Annals, **60**(2), 821-842,

[8] Zanini F, Pagani L, Savio E, Carmignato S, 2019 Characterisation of additively manufactured metal surfaces by means of X-ray computed tomography and generalised surface texture parameters. CIRP Annals, **68**(1), DOI: 10.1016/j.cirp.2019.04.074.

[9] Wits W W, Carmignato S, Zanini F, Vaneker T H J, 2016 Porosity testing methods for the quality assessment of selective laser melted parts. CIRP Annals - Manufacturing Technology, **65**(1),201-204, DOI: 10.1016/j.cirp.2016.04.054